JOC Article
pubs.acs.org/joc

Formation of Fullerooxazoles from $C_{61}HPh^{3-}$: The Regioselectivity of Heteroatom Additions

Fang-Fang Li,[†] Wei-Wei Yang,[†] Guo-Bao He,[‡] and Xiang Gao*,[†]

[†]*State Key Laboratory of Electroanalytical Chemistry, Changchun Institute of Applied Chemistry, Graduate School of Chinese Academy of Sciences, Chinese Academy of Sciences, 5625 Remin Street, Changchun, Jilin 130022, China, and* [‡]*Yichang Institute of Measurement and Testing Technology, Yichang 443003, China*

xgao@ciac.jl.cn

Received June 9, 2009

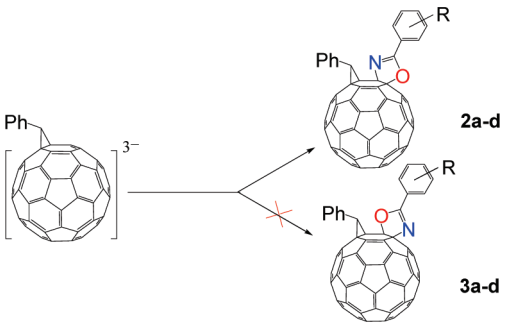

The formation of fullerooxazoles from $C_{61}HPh^{3-}$ has been examined in benzonitrile (PhCN), *m*-methoxybenzonitrile (*m*-OCH_3PhCN), *m*-tolunitrile (*m*-CH_3PhCN), and *o*-tolunitrile (*o*-CH_3PhCN), where *cis*-1 bisadducts with Ph-, *m*-OCH_3Ph-, *m*-CH_3Ph-, and *o*-CH_3Ph-substituted cyclic imidate next to the phenylmethano are formed as evidenced by various characterizations. Interestingly, only regioisomers **2a**−**d** with the oxygen atom bonded to C4/C5 and the nitrogen atom bonded to C3/C6 are generated as demonstrated by heteronuclear multiple bond coherence (HMBC) NMR, while the alternative regioisomers **3a**−**d**, which have the oxygen and nitrogen atoms at C3/C6 and C4/C5, respectively, are not formed from the reactions, even though the DFT (density functional theory) calculations have predicted that the energy differences between the two types of regioisomers are very small, with regioisomers **3a**−**d** actually having lower energies than **2a**−**d**. The results are rationalized by the charge distributions of $C_{61}HPh^{3-}$, where computational calculations have shown that the negative charges on C4 and C5 are greater than those on C3 and C6, indicating that the exhibited site selectivity of heteroatoms is a result of the charge-directed addition process.

Introduction

Reactions involving anionic C_{60} species have been very attractive, since unlike neutral C_{60}, which is electron deficient and acts as an electrophile,[1] anionic C_{60} is an electron donor and behaves as an nucleophile.[2] The chemistry of anionic C_{60} is an important complement to that of C_{60}, where protocols using dianionic C_{60} as a building block for fullerene functionalizations,[3] and retro-cycloaddition reactions of anionic fullerene derivatives as a synthetic tool for

(1) Hirsch, A.; Brettreich, M. *Fullerenes: Chemistry and Reactions*; Wiley-VCH Verlag GmbH & Co. KGaA: Weinheim, Germany, 2005.

(2) (a) Echegoyen, L.; Echegoyen, L. E. *Acc. Chem. Res.* **1998**, *31*, 593–601. (b) Reed, C. A.; Bolskar, R. D. *Chem. Rev.* **2000**, *100*, 1075–1120.

(3) (a) Caron, C.; Subramanian, R.; D'Souza, F.; Kim, J.; Kunter, W.; Jones, M. T.; Kadish, K. M. *J. Am. Chem. Soc.* **1993**, *115*, 8505–8506. (b) Boulas, P. L.; Zuo, Y.; Echegoyen, L. *Chem. Commun.* **1996**, 1547–1548. (c) Subramanian, R.; Kadish, K. M.; Vijayashree, M. N.; Gao, X.; Jones, M. T.; Miller, D. M.; Krause, K.; Suenobu, T.; Fukuzumi, S. *J. Phys. Chem.* **1996**, *100*, 16327–16335. (d) Fukuzumi, S.; Suenobu, T.; Hirasaka, T.; Arakawa, R.; Kadish, K. M. *J. Am. Chem. Soc.* **1998**, *120*, 9220–9227. (e) Kadish, K. M.; Gao, X.; Van Caemelbecke, E.; Hirasaka, T.; Suenobu, T.; Fukuzumi, S. *J. Phys. Chem. A* **1998**, *102*, 3898–3906. (f) Zhu, Y.-H.; Song, L.-C.; Hu, Q.-M.; Li, C.-M. *Org. Lett.* **1999**, *1*, 1693–1695. (g) Kadish, K. M.; Gao, X.; Van Caemelbecke, E.; Suenobu, T.; Fukuzumi, S. *J. Am. Chem. Soc.* **2000**, *122*, 563–570. (h) Allard, E.; Delaunay, J.; Cheng, F.; Cousseau, J.; Orduna, J.; Garin, J. *Org. Lett.* **2001**, *3*, 3503–3506. (i) Cheng, F.; Murata, Y.; Komatsu, K. *Org. Lett.* **2002**, *4*, 2541–2544. (j) Meier, M. S.; Bergosh, R. G.; Gallagher, M. E.; Spielmann, H. P.; Wang, Z. *J. Org. Chem.* **2002**, *67*, 5946–5952. (k) Wang, Z.; Meier, M. S. *J. Org. Chem.* **2003**, *68*, 3043–3048. (l) Allard, E.; Delaunay, J.; Cousseau, J. *Org. Lett.* **2003**, *5*, 2239–2242. (m) Zheng, M.; Li, F.; Shi, Z.; Gao, X.; Kadish, K. M. *J. Org. Chem.* **2007**, *72*, 2538–2542.

DOI: 10.1021/jo9012207 Published on Web 09/30/2009

SCHEME 1

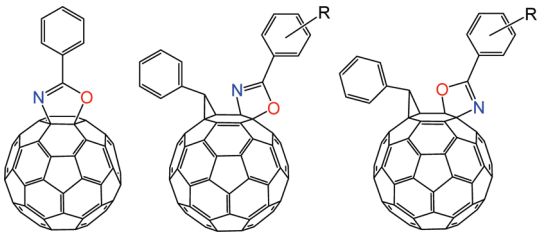

1 **2** **3**

a: R = H **a**: R = H

b: R = *m*-OCH_3 **b**: R = *m*-OCH_3

c: R = *m*-CH_3 **c**: R = *m*-CH_3

d: R = *o*-CH_3 **d**: R = *o*-CH_3

preparation of higher fullerene isomers[4] have been well established. In addition, recent work has shown that anionic C_{60} encapsulated in bicapped γ-cyclodextrins is capable of dinitrogen fixation in aqueous solution under mild conditions,[5] and the same species also exhibits an efficient catalytic reducing ability toward certain functional groups,[6] indicating that anionic C_{60} may possess more intriguing properties that need to be explored.

Compared to the work on dianionic C_{60},[3] study on the reactivity of trianionic C_{60} is very limited.[7] Recently, an unexpected reaction of trianionic C_{60} in deaerated benzonitrile solution leading to the formation of fullerooxazole, [6,6] cyclic phenylimidate C_{60} (**1** in Scheme 1) has been reported.[7d] However, there are still two puzzles remaining for the reaction. One is the origin of the oxygen atom for **1** from a system that was well deaerated, and the other is if there is regioselectivity for the addition of the heteroatoms. As for the current work, the focus is placed on the second one. Due to the high symmetry of the C_{60} molecule, it shows no regioselectivity for the addition of oxygen and nitrogen atoms on the C_{60} sphere in **1**, and the reaction leads to the formation of only one regioisomer.[7d] However, the scenario is quite different when a C_{60} derivative, such as phenylmethanofullerene (C_{61}HPh), is used as the staring material, where it would theoretically give rise to two types of regioisomers (**2** and **3** in Scheme 1) due to the lowering of molecular symmetry. It is therefore of interest to use trianionic C_{61}HPh instead of trianionic C_{60} to further probe the reaction, and to examine if there is regioselectivity for the addition of heteroatoms.

Results and Discussion

Procedures for producing fullerooxazole compounds from $C_{61}HPh^{3-}$ in PhCN, *m*-OCH_3PhCN, *m*-CH_3PhCN, and *o*-CH_3PhCN were similar to those reported previously,[7d] and details of the synthesis are described in the Experimental Section. A crude mixture containing individual fullerooxazole products was put into toluene and sonicated, and the soluble part was further purified by HPLC with use of a Buckyprep column. This shows only two major fractions in the HPLC trace for each synthesis (Figure S1 in the Supporting Information): one is the fullerooxazole product and the other is unreacted C_{61}HPh. Under typical conditions, the isolated yield for fullerooxazoles generated from PhCN, *m*-OCH_3PhCN, *m*-CH_3PhCN, and *o*-CH_3PhCN and is ca. 35%, 40%, 35%, and 4%, and there is ca. 15%, 18%, 15%, and 40% C_{61}HPh recovered from the respective reaction. The remainder of the crude mixture is insoluble in CS_2 or toluene; however, it is soluble in more polar solvent such as DMF or THF. MALDI FT-ICR MS (matrix-assisted laser desorption ionization Fourier transform ion cyclotron resonance mass spectrometry) of this residual material shows peaks corresponding to C_{60} and higher carbon clusters such as C_{110}, with no feature of oxazole adducts including mono-, di-, tri-, or polyadduct, indicating that there is no fullerooxazole compound in it.

The four isolated products generated from PhCN, *m*-OCH_3PhCN, *m*-CH_3PhCN, and *o*-CH_3PhCN are denoted as fullerooxazoles **Fa**, **Fb**, **Fc**, and **Fd**, respectively, which could in principle be either regioisomers **2** and/or **3**. Among them, single crystals suitable for X-ray diffraction were obtained for **Fa**. Figure 1 shows the X-ray single-crystal structure of **Fa** with partial atomic numbering. A five-membered heterocycle is present by bonding to C_{60}. The same heterocycle is also shown in the previously obtained crystal structure of 1,4-dibenzyl-2,3-cyclic phenylimidate C_{60},[7d] implying $C_{61}HPh^{3-}$ undergoes the same reaction as that of C_{60}^{3-} with PhCN. However, the exact position of the nitrogen or oxygen atom on the C_{60} sphere cannot be

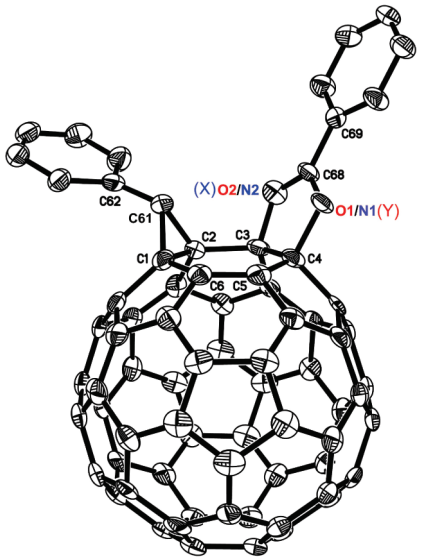

FIGURE 1. ORTEP drawing of **Fa**, which could be **2a** and/or **3a**, with 20% thermal ellipsoids. Hydrogen atoms are omitted for clarity. Selected bond distances (Å) and bond angles (deg): C1−C2, 1.584(8); C2−C3, 1.559(7); C3−C4, 1.582(7); C4−C5, 1.521(8); C5−C6, 1.358(7); C6−C1, 1.486(7); C3−X, 1.482(6); X−C68, 1.312(7); C68−Y, 1.320(6); Y−C4, 1.476(6); X−C68−Y, 118.9(4); X−C68−C69, 123.8(5); Y−C68−C69, 117.2(5).

(4) Herranz, M. Á.; Diederich, F.; Echegoyen, L. *Eur. J. Org. Chem.* **2004**, 2299–2316.

(5) (a) Nishibayashi, Y.; Saito, M.; Uemura, S.; Takekuma, S.; Takekuma, H.; Yoshida, Z. *Nature* **2004**, *428*, 279–280. (b) Pospíšil, L.; Bulíčková, J.; Hromadová, M.; Gál, M.; Ciciš, S.; Cihelka, J.; Tarábek, J. *Chem. Commun.* **2007**, *22*, 2270–2272.

(6) Takekuma, S.; Takekuma, H.; Yoshida, Z. *Chem. Commun.* **2005**, 1628–1630.

(7) (a) Dubois, D.; Kadish, K. M.; Flanagan, S.; Haufler, R. E.; Chibante, L. P. F.; Wilson, L. J. *J. Am. Chem. Soc.* **1991**, *113*, 4364–4366. (b) Khaled, M. M.; Carlin, R. T.; Trulove, P. C.; Eaton, G. R.; Eaton, S. S. *J. Am. Chem. Soc.* **1994**, *116*, 3465–3474. (c) Beulen, M. W. J.; Echegoyen, L. *Chem. Commun.* **2000**, 1065–1066. (d) Zheng, M.; Li, F.-F.; Ni, L.; Yang, W.-W.; Gao, X. *J. Org. Chem.* **2008**, *73*, 3159–3168.

differentiated unambiguously by crystallography due to the similar electron density of these two atoms. Both **2a** and **3a** fit well with the resolved crystal structure. The heteroatoms bonded to C3 and C4 are labeled as X and Y, respectively. Notably, the structure shown in Figure 1 is chiral with an enantiomer having the cyclic phenylimidate positioned at 5-Y-6-X, indicating that the isolated product is a racemic mixture.

The characterization of **Fa** was further carried out by negative MALDI FT-ICR MS (Figure S2 in the Supporting Information) with 2,5-dihydroxybenzoic acid (DHB) as the matrix. The monoisotopic molecular ion of the compound is shown at 929.08181, which has a deviation of only −3.0 ppm from the theoretical value of 929.08461 ($C_{74}H_{11}NO^-$), indicating that the compound has a formula of $C_{74}H_{11}NO$, consistent with the X-ray single-crystal results.

Although the chemical formula of **Fa** is $C_{74}H_{11}NO$, and the skeleton of the compound has a cyclic phenylimidate bonded to C_{60} via a nitrogen and an oxygen atom next to the phenylmethano group, it is not clarified yet as to how the heteroatoms of oxygen and nitrogen are positioned on C_{60}, since both regioisomers **2a** and **3a** fit well with the single-crystal structure. Computational calculations were carried out to evaluate the structures of the two isomers. The structures of **2a** and **3a** were optimized at the B3LYP/6-31G level with the Gaussian 03 program,[8] followed by harmonic frequency calculations with the same method to confirm them as energy minima. The selected bond lengths and bond angles for the optimized structures of **2a** and **3a**, along with those for the single crystal of the obtained product (**Fa**), are shown in the Supporting Information. The calculated total energies for **2a** and **3a** are −2955.49178 and −2955.49194 hartree/mol (1 hartree/mol = 627.5095 kcal/mol), respectively. The results predict that the two isomers have a very small energy difference, with isomer **3a** being about only 0.10 kcal/mol more stable than isomer **2a**, implying that both isomers could be formed if the reaction is only thermodynamically controlled. However, as the optimized structures are examined, the structure of **2a** has a better match with the crystal data. The bond angles of X−C68−C69 and Y−C68−C69 for **2a** are calculated to be 125.8° and 116.1°, consistent with the values of 123.8(5)° and 117.2(5)° observed for **Fa**, while the calculated values for the same angles of **3a** are 116.1° and 125.8°, which are opposite to the corresponding angles observed experimentally, suggesting that the obtained fullerooxazole **Fa** has the structure of **2a**.

The structural assignment of **Fa** is further explored with NMR spectroscopy. The ^{1}H NMR spectrum of **Fa** (see the Supporting Information) shows resonances corresponding to the phenyl protons of cyclic phenylimidate appearing at 8.42 (d, 2H), 7.65 (t, 1H), and 7.59 (t, 2H) ppm, and resonances from the phenyl protons of phenylmethano appearing at 7.62 (d, 2H), 7.33 (t, 2H), and 7.26 (t, 1H) ppm, while the singlet at 5.06 (s, 1H) ppm is due to the methine proton of the phenylmethano group. The ^{13}C NMR spectrum of the compound shows a total of 58 sp^2 carbons (see the Supporting Information). The most downfield one at 165.2 ppm is ascribed to the imine carbon of the cyclic phenylimidate, while 49 resonances from 154.9 to 137.1 ppm are due to the sp^2 C_{60} carbons, consistent with the C_1 symmetry of the molecule observed by X-ray single-crystal diffraction. The remaining eight peaks from 133.0 to 126.5 ppm are ascribed to the phenyl carbons of the phenylimidate and phenylmethano groups. As for the sp^3 carbons, the resonance at 44.3 ppm is from the methine carbon, and the two resonances at 65.1 and 61.9 ppm correspond to the sp^3 C_{60} carbons connected to the phenylmethano group. Two additional resonances are observed at 96.2 and 85.4 ppm, which are due to the sp^3 C_{60} carbons bonded to the heteroatoms of oxygen and nitrogen. The appearance of only one set of resonances in the ^{1}H and ^{13}C NMR spectra of the compound indicates that the obtained fullerooxazole has only one regioisomeric structure, i.e., either **2a** or **3a** is formed. Since the phenylmethano and phenylimidate are positioned next to each other with the *cis*-1 pattern, it is possible to reveal the identity of the heteroatoms bonded to C3 with HMBC NMR by examining the three-bond correlation ($^3J_{CH}$)[9] of the methine proton with C3 (refer to Figure 1 for labeling). In this case, the assignment of the two sp^3 C_{60} carbons bonded to the heteroatoms is crucial for the structural elucidation. Previous work on five-membered hetereocyclic C_{60} derivatives has shown that the resonance for the sp^3 C_{60} carbon atoms bonded to an oxygen atom ranges from about 104 to 96 ppm,[7d,10] while resonance for the sp^3 C_{60} carbon atoms bonded to a nitrogen atom ranges from about 100 to 80 ppm;[7d,10e,11] it is therefore rational to assign the resonance at 96.2 ppm to the C_{60} sp^3 carbon atom bonded to the oxygen atom, while the one at 85.4 ppm is assigned to the C_{60} sp^3 carbon atom bonded to the nitrogen atom. The assignment is also consistent with the fact that the electronegativity of the oxygen atom is greater than that of the nitrogen atom.

Figure 2 shows the HMBC spectrum of **Fa**. There is a cross peak between the methine proton and the C_{60} sp^3 carbon atom resonating at 86.0 ppm as indicated by the circle. The cross peak is a result of a three-bond correlation between the methine proton and the carbon atom (C3 as labeled in Figure 1) next to the phenylmethano, thus providing unambiguous evidence that C3 is bonded to the nitrogen atom. No correlation is observed between the methine proton and

(8) Frisch, M. J.; Trucks, G. W.; Schlegel, H. B.; Scuseria, G. E.; Robb, M. A.; Cheeseman, J. R.; Montgomery, J. A., Jr.; Vreven, T.; Kudin, K. N.; Burant, J. C.; Millam, J. M.; Iyengar, S. S.; Tomasi, J.; Barone, V.; Mennucci, B.; Cossi, M.; Scalmani, G.; Rega, N.; Petersson, G. A.; Nakatsuji, H.; Hada, M.; Ehara, M.; Toyota, K.; Fukuda, R.; Hasegawa, J.; Ishida, M.; Nakajima, T.; Honda, Y.; Kitao, O.; Nakai, H.; Klene, M.; Li, X.; Knox, J. E.; Hratchian, H. P.; Cross, J. B.; Bakken, V.; Adamo, C.; Jaramillo, J.; Gomperts, R.; Stratmann, R. E.; Yazyev, O.; Austin, A. J.; Cammi, R.; Pomelli, C.; Ochterski, J. W.; Ayala, P. Y.; Morokuma, K.; Voth, G. A.; Salvador, P.; Dannenberg, J. J.; Zakrzewski, V. G.; Dapprich, S.; Daniels, A. D.; Strain, M. C.; Farkas, O.; Malick, D. K.; Rabuck, A. D.; Raghavachari, K.; Foresman, J. B.; Ortiz, J. V.; Cui, Q.; Baboul, A. G.; Clifford, S.; Cioslowski, J.; Stefanov, B. B.; Liu, G.; Liashenko, A.; Piskorz, P.; Komaromi, I.; Martin, R. L.; Fox, D. J.; Keith, T.; Al-Laham, M. A.; Peng, C. Y.; Nanayakkara, A.; Challacombe, M.; Gill, P. M. W.; Johnson, B.; Chen, W.; Wong, M. W.; Gonzalez, C.; Pople, J. A. *Gaussian 03*, Revision D.01; Gaussian, Inc., Wallingford, CT, 2004.

(9) Silverstein, R. M.; Webster, F. X. *Spectrometric Identification of Organic Compounds*, 6th ed.; John Wiley & Sons, Inc.: New York, 1998; pp 263−268.

(10) (a) Meier, M. S.; Poplawska, M. *J. Org. Chem.* **1993**, *58*, 4524–4525. (b) Meier, M. S.; Poplawska, M. *Tetrahedron* **1996**, *52*, 5043–5052. (c) Wang, G.-W.; Li, F.-B.; Chen, Z.-X.; Wu, P.; Cheng, B.; Xu, Y. *J. Org. Chem.* **2007**, *72*, 4779–4783. (d) Wang, G.-W.; Li, F.-B.; Xu, Y. *J. Org. Chem.* **2007**, *72*, 4774–4778. (e) Liu, T.-X.; Wang, G.-W. *J. Org. Chem.* **2008**, *73*, 6417–6420.

(11) (a) Shen, C. K.-F.; Yu, H.-h.; Juo, C.-G.; Chien, K.-M.; Her, G.-R.; Luh, T.-Y. *Chem.—Eur. J.* **1997**, *3*, 744–748. (b) Delgado, J. L.; Cardinali, F.; Espíldora, E.; Torres, M. R.; Langa, F.; Martín, N. *Org. Lett.* **2008**, *10*, 3705–3708.

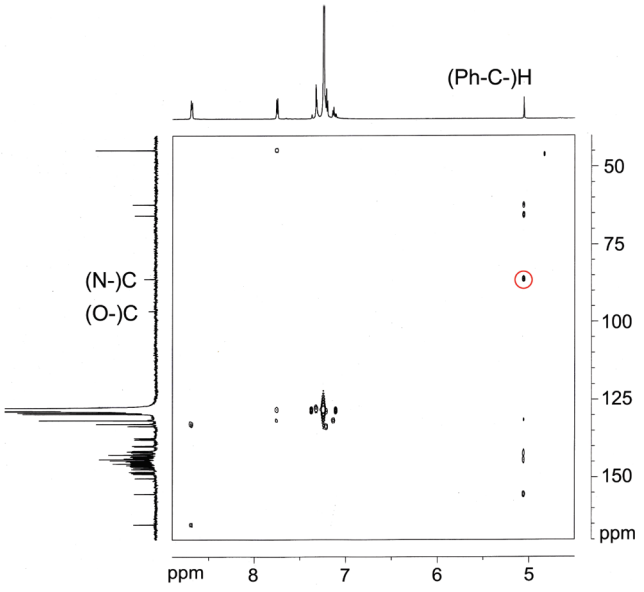

FIGURE 2. HMBC spectrum of **2a** in benzene-d_6.

the carbon atom resonating at 96.5 ppm, indicating that the carbon atom bonded to the oxygen atom has at least a four-bond coupling with the methine proton. On the basis of the crystal structure shown in Figure 1, C4 is bonded to the oxygen atom. The structure of the fullerooxazole **Fa** obtained from $C_{61}HPh^{3-}$ benzonitrile solution is therefore identified unequivocally to be **2a**.

To further confirm that only **2a** is formed, while **3a** is not formed from the reaction, the initial crude reaction mixture was subjected to ^{1}H NMR characterization directly (Figure S3 in the Supporting Information) to exclude the possibility that **3a** might be retained on the HPLC column under the experimental conditions. The spectrum is too complicated for a complete elucidation due to the peak overlapping caused by the presence of several compounds; however, it is still possible to discern the presence of only one fullerooxazole in the reaction mixture. The doublet at 8.18 ppm corresponds to *o*-H of the cyclic imidate phenyl. The appearance of only one set of this doublet is a strong indication that only one fullerooxazole is formed. Resonances around 5 ppm are due to the methine protons of phenylmethano, where the peak at 4.809 ppm is due to the methine proton of the oxazole product as compared with the spectra of **Fb-d** in the same solvent system, while the one at 5.135 ppm is from unreacted $C_{61}HPh$. The small resonance at 4.883 ppm may raise concerns about the possible existence of other fullerooxazole compounds in the mixture; however, the lack of the corresponding oxazole phenyl protons in the downfield region, and the perfect 2:1 area ratio of the doublet at 8.18 ppm with the singlet at 4.809 ppm indicate that the small singlet at 4.883 ppm is not from any fullerooxazole product, but likely corresponds to a small amount of unknown product that possesses phenylmethano, which is eluted out from the HPLC column as a small unidentified fraction as shown in Figure S1 (Supporting Information). The results confirm that only **2a** is generated from the reaction, while no **3a** is formed.

It is surprising that only regioisomer **2a** is formed from the reaction of $C_{61}HPh^{3-}$ in benzonitrile, since theoretical calculations predict a very small energy difference between **2a** and **3a**, especially when considering that **3a** is actually slightly energetically favored over **2a**. It is therefore of interest to probe further into the reaction to examine the generality of such regioselectivity. For this purpose, the reactions of $C_{61}HPh^{3-}$ in three other nitriles, *m*-OCH_3PhCN, *m*-CH_3PhCN, and *o*-CH_3PhCN, were used. The work-up for the preparation and isolation of **Fb**, **Fc**, and **Fd** resembles those of **Fa** (**2a**). The yield for **Fd** is very low under typical conditions, probably due to the steric and/or electronic effect associated with the substituents at the ortho-position, while the yields for **Fb** and **Fc** are similar to that of **2a**. The HPLC traces for the purification of **Fb**, **Fc**, and **Fd** are shown in the Supporting Information.

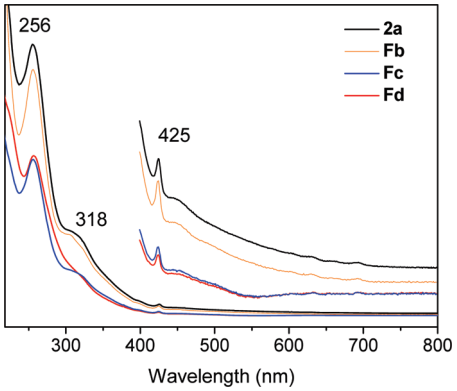

FIGURE 3. UV−vis spectra of **2a**, **Fb**, **Fc**, and **Fd** in hexane.

The chemical compositions of **Fb**, **Fc**, and **Fd** were revealed with negative ESI (electrospray ionization) FT-ICR MS (Figure S4 in the Supporting Information). The monoisotopic molecular ion for each compound is located at 959.09033, 943.09733, and 943.10293, respectively, which deviate from the theoretical value by only −5.1 ppm Da (**Fb**, $C_{75}H_{13}NO_2^-$, 959.09518) and −3.1 and 2.8 ppm Da (**Fc** and **Fd**, $C_{75}H_{13}NO^-$, 943.10026), indicating that the three compounds are all fullerooxazoles with the formula $C_{75}H_{13}NO_2$ for **Fb** and $C_{75}H_{13}NO$ for **Fc** and **Fd**. Notably, adduct ions of $[M + CH_3O]^-$ (*m*/*z* 990.10888, 974.11471, 974.11927) are all observed in the MS spectra of the three compounds, where CH_3O comes from the methanol that was used for ESI spraying.

It is expected that **Fb**, **Fc**, and **Fd** should also be *cis*-1 bisadducts like **2a** since *cis*-1 bisadduct is one of the most favorable regioisomers for bisadducts,[12] and such expectation is proved by the comparison of the UV−vis spectra of the four compounds. It has been shown that the UV−vis absorptions of [60]fullerene bisadducts are sensitive toward the addition pattern rather than the type of addends,[13] therefore the UV−vis is a powerful tool in determining the addition pattern of C_{60} bisadducts. Figure 3 displays the UV−vis spectra of **Fb**, **Fc**, and **Fd**, along with the spectrum of **2a** for comparison. It shows that the UV−vis spectra of **Fb**, **Fc**, and **Fd** are similar to that of **2a**, with a strong absorption

(12) Hirsch, A. *Top. Curr. Chem.* **1999**, *199*, 1–65.
(13) (a) Djojo, F.; Herzog, A.; Lamparth, I.; Hampel, F.; Hirsch, A. *Chem.—Eur. J.* **1996**, *2*, 1537–1547. (b) Nakamura, Y.; Takano, N.; Nishimura, T.; Yashima, E.; Sato, M.; Kudo, T.; Nishimura, J. *Org. Lett.* **2001**, *3*, 1193–1196. (c) Kordatos, K.; Bosi, S.; Da Ros, T.; Zambon, A.; Lucchini, V.; Prato, M. *J. Org. Chem.* **2001**, *66*, 2802−2808 and references cited therein.

at 256 nm, and a spike at 425 nm, which is characteristic of *cis*-1 bisadducts,[13] indicating that **Fb**, **Fc**, and **Fd** are *cis*-1 bisadducts.

However, like the case for the reaction in PhCN, there are also two likely regioisomers for the product obtained from *m*-OCH_3PhCN, *m*-CH_3PhCN, and *o*-CH_3PhCN (**2b**−**d** versus **3b**−**d**). Computational calculations with the Gaussian 03 program at the B3LYP/6-31G level predict that the energy differences between the two types of regioisomers are very small (**2b**: −3069.97530 hartree/mol and **3b**: −3069.97579 hartree/mol; **2c**: −2994.80039 and **3c**: −2994.80049 hartree/mol; **2d**: −2994.79752 and **3d**: −2994.79779 hartree/mol), with isomers **3b**, **3c**, and **3d** being 0.31, 0.06, and 0.17 kcal/mol lower than isomers **2b**, **2c**, and **2d**, respectively. The results therefore suggest that both types of isomers (**2** and **3**) are likely to be formed since the energy difference between them is small.

The structural elucidations of **Fb**, **Fc**, and **Fd** are further explored with NMR spectroscopy. The ^{1}H NMR spectra of the three compounds (Supporting Information) are in good agreement with the structural assignment, while the ^{13}C NMR spectra are also consistent with the structural assignment except that the resonances corresponding to the sp^3 C_{60} carbon atoms bonded to the heteroatoms for **Fd** are not resolved, probably due to the inherent low NMR sensitivity of these two carbon atoms and also the low yield of the compound. Fortunately, the lack of these two resonances in the ^{13}C NMR does not hamper the final structural assignment for **Fd** with HMBC NMR as shown below, since the missed resonance of the carbon atom bonded to the nitrogen atom appears at 85.5 ppm by showing a correlation peak with the methine proton in the HMBC spectrum, which is probably due to the sensitivity enhancement caused by the proton-detected technique used for HMBC.[9] Like the case of **2a**, there is only one set of NMR resonances for **Fb**, **Fc**, and **Fd**, indicating that only one of the two likely regioisomers is formed, and it has to rely on the HMBC NMR, where correlations between the methine proton and the sp^3-C of C_{60} bonded to heteroatoms are crucial, to reveal the identity of **Fb**, **Fc**, and **Fd**. Figure 4 shows HMBC NMR of **Fb**, **Fc**, and **Fd**. Cross peaks between the methine proton and the carbon atom resonating at 84.8, 84.8, and 85.5 ppm are shown as indicated by the circle for **Fb**, **Fc**, and **Fd**, respectively. The resonance around 85 ppm is due to the sp^3-C of C_{60} bonded to the nitrogen atom according to the arguments discussed above, and the observed cross peak is a three-bond correlation ($^3J_{CH}$) between the methine proton and the C3 as is the case for **2a** (see Figure 1 for the carbon labeling). Therefore, it is clarified that the C3 in **Fb**, **Fc**, and **Fd** is bonded to the nitrogen atom, showing unambiguously that the obtained fullerooxazoles are **2b**−**d**, respectively, while regioisomers of **3b**−**d** are not formed.

Along with the results for **2a**, it shows that there is indeed a regioselectivity for the heteroatom additions on the C_{60} skeleton during the formation of fullerooxazoles from $C_{61}HPh^{3-}$. Since the energy difference between the two types of isomers **2** and **3** is very small, and especially that **3** actually has a lower energy value than **2** according to DFT calculations, it is surprising to find that only regioisomers **2a**−**d** are formed experimentally. In fact, a similar situation has been observed during the study of methanofullerenes and fulleroids. It shows that even though methanofullerenes are calculated to be energetically favored by as much as

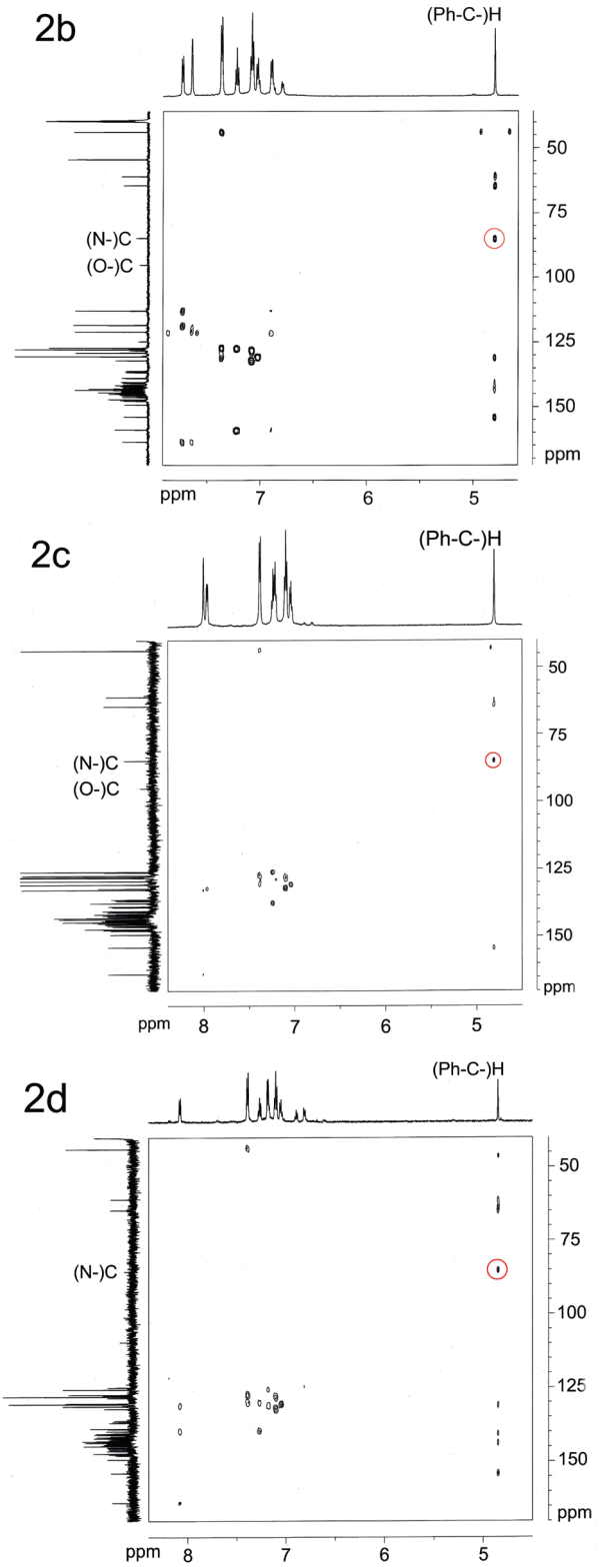

FIGURE 4. HMBC spectra of **2b**, **2c**, and **2d** in CS_2 with DMSO-d_6 as the external lock.

6 kcal/mol over fulleroids,[14] fulleroids can still be the major or exclusive product in reactions that are kinetically controlled,[15] suggesting that the fullerooxazole formation

(14) Raghavachari, K.; Sosa, C. *Chem. Phys. Lett.* **1993**, *209*, 223–228.

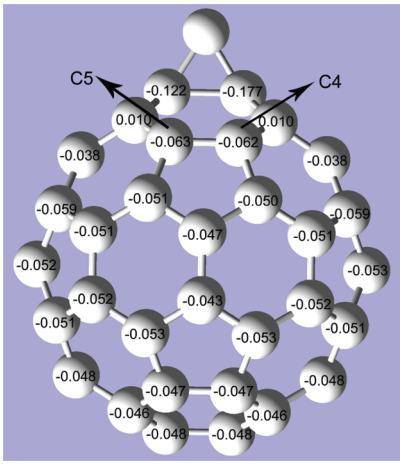

FIGURE 5. Calculated Mulliken charge distributions for $C_{61}HPh^{3-}$. Only half of the sphere to which the cyclic phenylimidate is added is shown. The phenylmethano group is omitted for clarity. See the Supporting Information for the other half sphere.

reaction involving the anionic C_{60} species is likely kinetically controlled. Previous work has shown that only trianion C_{60} is capable of initiating the reaction, while the neutral, mono- and dianionic C_{60} are unable to start the reaction,[7d] indicating that the amount of negative charge on the C_{60} skeleton is a crucial factor for the reaction. Figure 5 displays the Mulliken charge distributions of $C_{61}HPh^{3-}$ obtained at the B3LYP/6-31G theoretical level with the Gaussian 03 program. It shows that the largest charge is located at C4 and C5, which are the sites bonding to the oxygen atom, indicating that the addition of the oxygen atom is a charge-directed process during the fullerooxazole formation. Considering the fact that benzonitrile has a wide electrochemical window with $E_{1/2} = -2.17$ V versus SCE,[16] while the electrolysis potential for fullerooxazole synthesis is set at only -1.20 V versus SCE under deaerated conditions, it is unlikely that benzonitrile would be electrolyzed and form an oxygen-containing intermediate, which would then react with anionic C_{60} species via the 1,3-dipolar reaction[17] to form the product. In addition, it is also unlikely that anionic C_{60} would attack the nitrile molecule directly, since in that case, a C−C bond would form in the product due to the partial positive charge of the carbon atom in C≡N. Therefore it is reasonable to speculate that the reaction takes place via a stepwise procedure, where the charge-directed addition of the oxygen atom at C4/C5 is the first step to afford an intermediate, followed by a nucleophilic attack to the benzonitrile molecule of this intermediate to form regioisomers **2a**−**d**. The results imply that the oxygen atom in the products is likely electrophilic during the reaction.

Conclusion

In summary, the recently discovered reaction of trianionic C_{60} leading to the formation of fullerooxazoles has been further studied by using $C_{61}HPh^{3-}$ in benzonitrile, *m*-methoxybenzonitrile, *m*-tolunitrile, and *o*-tolunitrile. The reaction can theoretically lead to the formation of two types of possible regioisomers, **2** and **3**, due to the symmetry lowering of $C_{61}HPh^{3-}$. However, only regioisomers **2a**−**d** are obtained, although the alternative isomers **3a**−**d** are slightly energetically favorable as predicted by DFT calculations. Such regioselectivity for the formation of fullerooxazoles can be well rationalized by the charge distributions on $C_{61}HPh^{3-}$, where the site for the oxygen addition has the largest negative charge, implying that the oxygen atom in the products is likely electrophilic during the reaction, and the addition of the oxygen atom is a charge-directed process, which is likely the first step for the reaction. The results provide further information on the reactivity of trianionic C_{60}, which represents a largely unexplored field at the present time.

Experimental Section

Synthesis of 2a−**d.** Procedures for the generation of **2a**,**c**,**d** are similar to those reported previously.[7d] Typically $C_{61}HPh$ (50 mg, 61.7 μmol), which was obtained by the reaction of C_{60} dianion with benzal bromide ($PhCHBr_2$) according to the previous methods,[3m] was electrolyzed at -1.20 V versus SCE in 50 mL of freshly distilled nitrile solution (PhCN, *m*-CH_3PhCN, or *o*-CH_3PhCN) containing 0.1 M tetra-*n*-butylammonium perchlorate (TBAP) under an argon atmosphere. The reducing potential was continuously applied until an extra irreversible anodic wave appeared at ca. -0.54 V versus SCE in addition to the redox waves of $C_{61}HPh$ as examined by cyclic voltammetry (CV). The resulting anionic $C_{61}HPh$ nitrile solution was kept under stirring for 30 min, followed by electrochemical oxidization to the neutral form with a potential of 0 V versus SCE. The procedures for the generation of **2b** are similar to those of **2a**,**c**,**d**, except the nitrile solution (*m*-OCH_3PhCN) was used as received.

The solvent was removed with a rotary evaporator under reduced pressure after the reaction for **2a**,**c**,**d** was finished, and the residue was washed with methanol to remove TBAP before further purification. A large amount of methanol was put into the reaction mixture of **2b** directly to precipitate the product. The slurry was separated by filtration, and the residue was put into toluene and sonicated. The soluble part was further purified by HPLC, using a Buckyprep column (see the Supporting Information).

Spectral Characterization of 2a. Negative MALDI FT-ICR MS, *m*/*z* calcd for $C_{74}H_{11}NO$ $[M]^-$ 929.08461, found 929.08181; ^{1}H NMR (600 MHz, CS_2/$CDCl_3$) δ 8.42 (d, 2H), 7.65 (t, 1H), 7.62 (d, 2H), 7.59 (t, 2H), 7.33 (t, 2H), 7.26 (t, 1H), 5.06 (s, 1H); ^{13}C NMR (150 MHz, $CDCl_3$) δ 165.2 (1C, C=N), 154.9 (1C), 150.1 (1C), 148.7 (1C), 148.4(1C), 148.3 (1C), 148.0 (1C), 148.0 (1C), 147.1 (1C), 146.8 (1C), 146.4 (1C), 146.2 (1C), 146.0 (1C), 145.9 (1C), 145.8 (1C), 145.5 (1C), 145.4 (2C), 145.3 (1C), 145.3 (1C), 145.1 (1C), 144.9 (1C), 144.8 (1C), 144.5 (1C), 144.4 (3C), 144.3 (2C), 144.3 (1C), 143.9 (3C), 143.7 (1C), 143.7 (1C), 143.6 (1C), 143.3 (1C), 143.1 (1C), 143.0 (1C), 142.8 (1C), 142.6 (1C), 142.5 (1C), 142.4 (1C), 142.4 (1C), 142.2 (1C), 141.7 (1C), 141.4 (1C), 141.3 (1C), 141.3 (2C), 141.1 (1C), 139.8 (1C), 139.5 (1C), 139.4 (1C), 137.4 (1C), 137.4 (1C), 137.0 (1C), 133.0(1C, Ph), 132.8 (1C, Ph), 131.2 (2C, Ph), 129.3 (2C, Ph), 128.9 (2C, Ph), 128.5 (2C, Ph), 127.9 (1C, Ph), 126.5 (1C, Ph), 96.2 (1C, sp^3, C−O), 85.4 (1C, sp^3, C−N), 65.1 (1C, sp^3, C−CHC_6H_5), 61.9 (1C, sp^3, C−CHC_6H_5), 44.3 (1C, C−HC_6H_5); UV−vis (hexane) λ_{max}/nm 256, 318, and 425.

Spectral Characterization of 2b. Negative ESI FT-ICR MS, *m*/*z* calcd for $C_{75}H_{13}NO_2$ $[M]^-$ 959.09518, found 959.09033; ^{1}H

(15) (a) Suzuki, T.; Li, Q.; Khemani, K. C.; Wudl, F. *J. Am. Chem. Soc.* **1992**, *114*, 7301–7302. (b) Wudl, F. *Acc. Chem. Res.* **1992**, *25*, 157–161. (c) Prato, M.; Li, Q. C.; Wudl, F. *J. Am. Chem. Soc.* **1993**, *115*, 1148–1150. (d) Nakamura, Y.; Inamura, K.; Oomuro, R.; Laurenco, R.; Tidwellb, T. T.; Nishimura, J. *Org. Biomol. Chem.* **2005**, *3*, 3032–3038.

(16) Kojima, H.; Bard, A. J. *J. Am. Chem. Soc.* **1975**, *97*, 6317–6324.

(17) (a) Maggini, M.; Scorrano, G.; Prato, M. *J. Am. Chem. Soc.* **1993**, *115*, 9798–9799. (b) Prato, M.; Maggini, M. *Acc. Chem. Res.* **1998**, *31*, 519–526.

NMR (600 MHz, CS_2, DMSO-d_6 as the external lock) δ 7.73 (d, 1H), 7.64 (s, 1H), 7.37(d, 2H), 7.22 (t, 1H), 7.08 (t, 2H), 7.02 (t, 1H), 6.90 (d, 1H), 4.80 (s, 1H), 3.71 (s, 3H); ^{13}C NMR (150 MHz, CS_2, DMSO-d_6 as the external lock) δ 163.7 (1C, C=N), 159.0 (1C), 153.9 (1C), 149.3 (1C), 147.8(1C), 147.6 (1C), 147.5 (1C), 147.2 (2C), 146.3 (1C), 146.0 (1C), 145.6 (1C), 145.4 (1C), 145.3 (1C), 145.1 (2C), 144.8 (1C), 144.8 (1C), 144.6 (2C), 144.5 (1C), 144.4 (1C), 144.2 (1C), 144.0 (1C), 143.8 (2C), 143.6 (1C), 143.5 (3C), 143.5 (1C), 143.2 (2C), 143.0 (1C), 143.0 (1C), 142.9 (1C), 142.7 (1C), 142.4 (1C), 142.1 (1C), 142.1 (1C), 141.9 (1C), 141.8 (1C), 141.7 (1C), 141.7 (1C), 141.5 (1C), 141.0 (1C), 140.8 (1C), 140.7 (1C), 140.5 (1C), 140.5 (1C), 140.4 (1C), 139.1 (1C), 138.9 (1C), 138.8 (1C), 136.8 (1C), 136.4 (1C), 136.2 (1C), 132.1 (1C, Ph), 130.5 (2C, Ph), 129.1 (1C, Ph), 128.4 (1C, Ph), 127.9 (2C, Ph), 127.6 (1C, Ph), 127.3 (1C, Ph), 121.1 (1C, Ph), 118.5 (1C, Ph), 113.0 (1C), 95.2 (1C, sp^3, C−O), 84.8 (1C, sp^3, C−N), 64.4 (1C, sp^3, C−CHC_6H_5), 61.0 (1C, sp^3, C−CHC_6H_5), 54.4 (1C, sp^3, C−$CH_3OC_6H_5$), 43.8 (1C, sp^3 C−HC_6H_5); UV−vis (hexane) λ_{max}/nm 256, 318, and 425.

Spectral Characterization of 2c. Negative ESI FT-ICR MS, m/z calcd for $C_{75}H_{13}NO$ $[M]^-$ 943.10026, found 943.09733; ^{1}H NMR (600 MHz, CS_2, DMSO-d_6 as the external lock) δ 8.00 (s, 1H), 7.96 (d, 1H), 7.38 (d, 2H), 7.25−7.20 (m, 2H), 7.10 (t, 2H), 7.04 (t, 1H), 4.81 (s, 1H), 2.33 (s, 3H); ^{13}C NMR (150 MHz, CS_2, DMSO-d_6 as the external lock) δ 163.8 (1C, C=N), 154.0 (1C), 149.3 (1C), 147.8 (1C), 147.6 (1C), 147.5 (1C), 147.2 (2C), 146.3 (1C), 146.0 (1C), 145.6 (1C), 145.4 (1C), 145.3 (1C), 145.1 (1C), 145.1 (1C), 144.8 (1C), 144.8 (1C), 144.6 (2C), 144.5 (1C), 144.4 (1C), 144.2 (1C), 144.0 (1C), 143.9 (1C), 143.8 (1C), 143.6 (2C), 143.6 (2C), 143.5 (1C), 143.2 (2C), 143.0 (2C), 142.9 (1C), 142.7 (1C), 142.4 (1C), 142.1 (1C), 142.1 (1C), 141.9 (1C), 141.8 (1C), 141.8 (1C), 141.7 (1C), 141.5 (1C), 141.0 (1C), 140.9 (1C), 140.9 (1C), 140.5 (1C), 140.5 (1C), 139.1 (1C), 138.9 (1C), 138.8 (1C), 137.6 (2C), 136.8 (1C), 136.5 (1C), 136.2 (1C), 132.6 (1C, Ph), 132.1 (1C, Ph), 130.6 (2C, Ph), 129.3 (1C, Ph), 128.1 (1C, Ph), 127.9 (3C, Ph), 127.3 (1C, Ph), 126.1 (1C, Ph), 125.9 (1C, Ph), 95.1 (1C, sp^3, C−O), 84.8(1C, sp^3, C−N), 64.5 (1C, sp^3, C−CHC_6H_5), 61.0 (1C, sp^3, C−CHC_6H_5), 43.8 (1C, sp^3 C−HC_6H_5), 21.1(1C, sp^3, CH_3); UV−vis (hexane) λ_{max}/nm 256, 318, and 425.

Spectral Characterization of 2d. Negative ESI FT-ICR MS, m/z calcd for $C_{75}H_{13}NO$ $[M]^-$ 943.10026, found 943.10293; ^{1}H NMR (600 MHz, CS_2, DMSO-d_6 as the external lock) δ 8.08 (d, 1H), 7.39 (d, 2H), 7.27 (t, 1H), 7.18 (t, 2H), 7.10 (t, 2H), 7.05 (t, 1H), 4.85 (s, 1H), 2.82 (s 3H); ^{13}C NMR (150 MHz, CS_2, DMSO-d_6 as the external lock) δ 163.8 (1C, C=N), 153.9 (1C), 149.3 (1C), 147.9 (1C), 147.6 (1C), 147.6 (1C), 147.2 (2C), 146.4 (1C), 146.0 (1C), 145.6 (1C), 145.5 (1C), 145.3 (1C), 145.2 (1C), 145.1 (1C), 144.8 (3C), 144.6 (1C), 144.6 (1C), 144.5 (1C), 144.4 (1C), 144.2 (1C), 144.0 (1C), 143.9 (1C), 143.8 (1C), 143.6 (1C), 143.6 (1C), 143.5 (2C), 143.2 (3C), 143.0 (1C), 143.0 (1C), 143.0 (1C), 142.7 (1C), 142.4 (1C), 142.2 (2C), 141.9 (1C), 141.9 (1C), 141.8 (2C), 141.5 (1C), 141.0 (1C), 140.9 (2C), 140.6 (1C), 140.4 (1C), 139.8 (1C), 139.1 (1C), 138.9 (2C), 136.8 (1C), 136.5 (1C), 136.2 (1C), 132.1 (1C, Ph), 131.3 (1C, Ph), 131.2 (1C, Ph), 130.5 (2C, Ph), 130.3 (1C, Ph), 128.4 (1C, Ph), 127.9 (2C, Ph), 127.7 (1C, Ph), 127.3 (1C, Ph), 125.5 (1C, Ph), 85.5 (1C, sp^3, C−N), 64.6 (1C, sp^3, C−CHC_6H_5), 60.9 (1C, sp^3, C−CHC_6H_5), 43.9 (1C, sp^3, C−HC_6H_5), 22.9 (1C, sp^3, CH_3); UV−vis (hexane) λ_{max}/nm 256, 318, and 425.

X-ray Crystallographic Data Collection and Structure Refinement. Black lamellar crystals of compound **2a** suitable for an X-ray analysis were obtained by slowly diffusing hexane into a CS_2 solution of compound **2a** at room temperature. Single-crystal X-ray diffraction data were collected on a Bruker SMART Apex equipped with a CCD area detector, using graphite-monochromated Mo Kα radiation (λ = 0.71073 Å) in the scan range $1.54° < \theta < 26.07°$. The structure was solved with the direct methods by using the SHELXS-97[18] program and refined with full-matrix least-squares techniques using the SHELXL-97 program[19] within WINGX.[20] Non-hydrogen atoms were refined anisotropically. Crystal data of **2a**·0.5CS_2: $C_{74.50}H_{11}NOS$, M_w = 967.90, dark brown, orthorhombic, space group *Pbca*, a = 10.018(1) Å, b = 26.454(3) Å, c = 29.788(3) Å, α = 90.000°, β = 90.000°, γ = 90.000°, V = 7894.3(14) Å^3, z = 8, D_{calc} = 1.629 Mg m^{-3}, μ = 0.147 mm^{-1}, T = 187(2) K, crystal size 0.419 × 0.231 × 0.052 mm; reflections collected 39277, independent reflections 7309, 2887 with $I > 2\sigma(I)$; R_1 = 0.0817 [$I > 2\sigma(I)$], wR_2 = 0.1731 [$I > 2\sigma(I)$]; R_1 = 0.2060 (all data), wR_2 = 0.2321 (all data), GOF (on F^2) = 0.928.

Quantum Computational Methods. The Gaussian full geometry optimizations of **2a**−**d** and **3a**−**d** were performed by using the B3LYP functional and 6-31G basis set in the Gaussian 03 program package, followed by harmonic frequency calculations at the same level to confirm them as the energy minima. The geometry optimization and the Mulliken charge distribution analysis for the $C_{61}HPh$ trianion were performed with use of B3LYP/6-31G.

Acknowledgment. We thank Prof. Zhijian Wu and Dr. Meiyan Wang for helpful discussions on computational calculations. We also thank Prof. David I. Schuster at New York University for discussions regarding the numbering of the compounds. The work was supported by the National Natural Science Foundation of China (Grant No. 20972150) and the State Key Laboratory of Electroanalytical Chemistry of China.

Supporting Information Available: X-ray crystallographic files for **2a** (CIF), general methods, HPLC traces for purification of **2a**−**d**, experimental and calculated bond lengths and bond angles for **2a** and **3a**, ^{1}H NMR spectrum of the initial crude reaction mixture of **Fa**, ^{1}H and ^{13}C NMR spectra of **2a**−**d**, and DFT-optimized Cartesian coordinates of the molecules **2a**−**d** and **3a**−**d** and trianionic $C_{61}HPh$. This material is available free of charge via the Internet at http://pubs.acs.org.

(18) Sheldrick, G. M. *SHELXS-97*, A Program for Automatic Solution of Crystal Structure; University of Göttingen, Göttingen, Germany, 1997.
(19) Sheldrick, G. M. *SHELXL-97*, A Program for Crystal Structure Refinement; University of Göttingen, Göttingen, Germany, 1997.
(20) Farrugia, L. J. *WINGX*, A Windows Program for Crystal Structure Analysis; University of Glasgow, Glasgow, UK, 1988.